Electronic supplementary Information (ESI †) for

The Effect of Energetically Coated ZrO_x on Enhanced Electrochemical Performances of $Li(Ni_{1/3}Co_{1/3}Mn_{1/3})O_2$ Cathodes Using Modified Radio Frequency (RF) Sputtering

Ji-Hoon Lee,[a] Ji Woo Kim,[b,c] Ho-Young Kang,[a] Seul Cham Kim,[a] Sang Sub Han,[a] Kyu Hwan Oh,[a] Se-Hee Lee[*b], and Young-Chang Joo[*a,d]

[a] Dept. of Materials Science & Engineering, Seoul National University, Seoul 151-744, Korea

[b] Dept. of Mechanical Engineering, University of Colorado at Boulder, Boulder, CO 80300-0427, USA

[c] Battery R&D Division, LG Chem. Ltd, Research Park, 188 Munji-ro, Yu-Seong gu, Daejeon 305-783, Korea

[d] Research Institute of Advanced Materials (RIAM), Seoul National University, Seoul 151-742, Korea

Corresponding Authors

Young-Chang Joo (ycjoo@snu.ac.kr, Tel.: +82-2-880-8986)

Se-Hee Lee (sehee.lee@colorado.edu, Tel.: +1-303-492-7889)

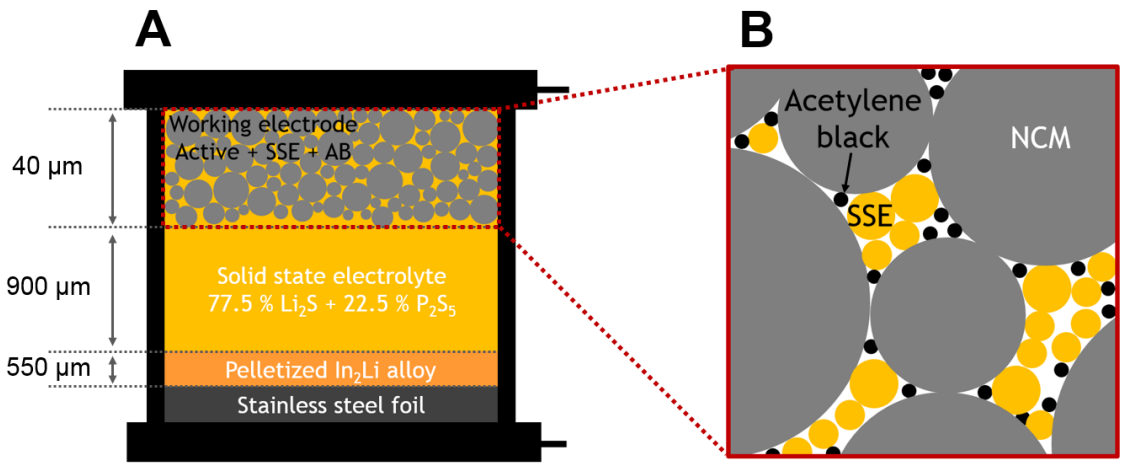

Schematic S1 (A) Schematic representation of the configuration of the all-solid-state cell (the thickness of each layer is denoted on the left side of the figure). (B) Composite working electrode composed of L333, solid-state electrolyte (SSE), and acetylene black.

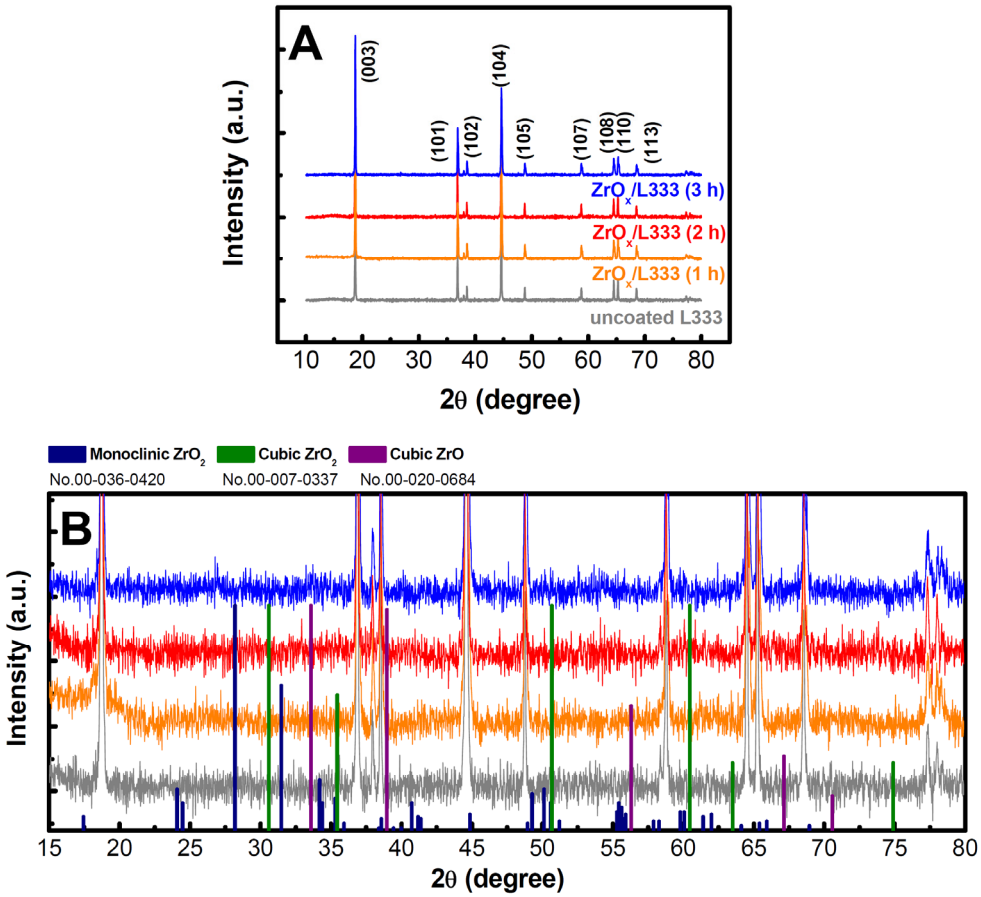

Fig. S1 (A) XRD patterns of uncoated and ZrO_x-coated (1, 2, and 3 h) L333 powders. (B) Magnified XRD patterns with a range of diffraction angle (2Θ) between 15 and 80° and bar-type peaks of monoclinic ZrO_2, cubic ZrO_2, and cubic ZrO_2 from the JCPDS card No.00-036-0420, No.00-007-0337, and No.00-020-0684, respectively.

Fig. S1 displays the XRD patterns of uncoated and ZrO_x-coated NCM333 powders as a function of sputtering time. Peak position related to lattice parameters is identical in all of powders investigated. It indicated that ZrO_x layer deposited at room temperature did not alter the structure of L333 or penetrate to inside of NCM333. All peaks detected were indexed as the hexagonal α-$NaFeO_2$ with a space group of R-3m[1,2]. It is well-known that the ratio of peak intensity, I(003)/I(104), is an indicator of the degree of

cation mixing and low degree of that occurred when the ratio is larger than 1.2[3]. The ratio for uncoated, 1, 2, and 3 h ZrO_x-coated L333 are 1.55, 1.65, 1.55, and 1.59, respectively. Fig. S1B shows the comparison of the measured diffraction patterns and standard diffraction patterns of ZrO_x (monoclinic ZrO_2, cubic ZrO_2, and cubic ZrO). Sputtering process occurred with physical atomic bombardment of sputtered atoms or molecules with randomly distributed sputtering direction. Therefore, based on the characteristic of sputtering and resulting XRD patterns, we concluded that ZrO_x coated at the surface and doped in the bulk region existed as amorphous structure

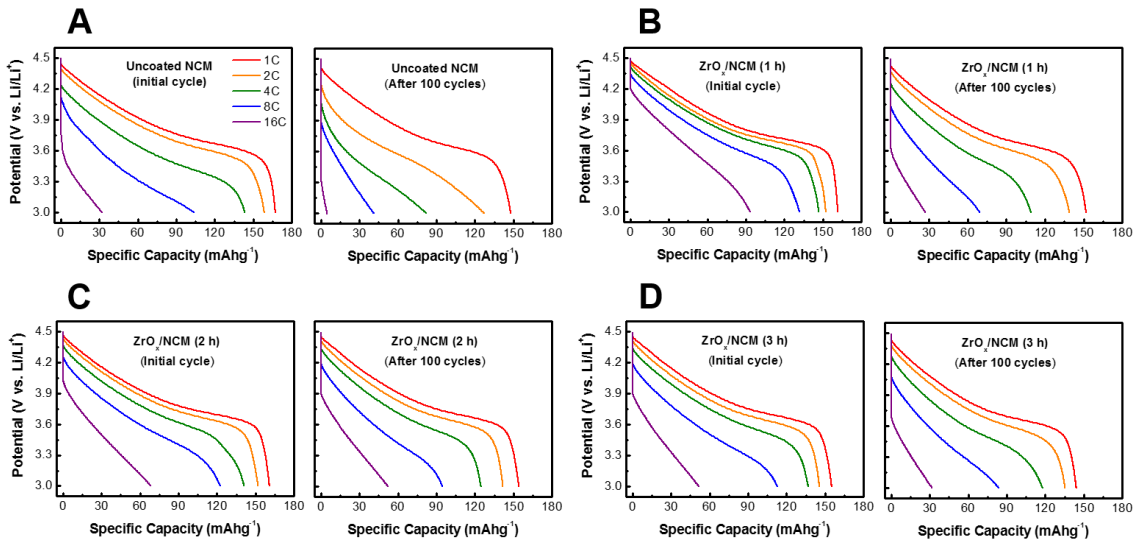

Fig. S2 Potential profiles as a function of C-rate evolved during discharge observed at 2 different ranges of the cycle number (initial cycle and after 100 cycles) for uncoated (A) and ZrO_x-coated L333 cathodes for 1 (B), 2 (C), and 3 h (D).

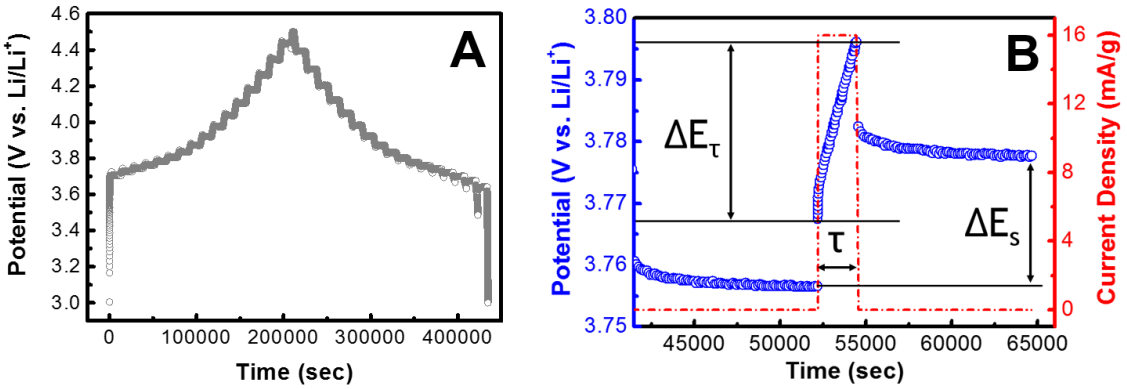

Fig. S3 (A) Potential changes of uncoated L333 electrodes measured using GITT within the potential range of 3.0 to 4.5 V (vs. Li/Li^+). (B) Single titration curves for potential change and applied charging current density. The denoted parameters (ΔE_τ, τ, and ΔE_s) were used in the calculation of the diffusion coefficient of Li ions.

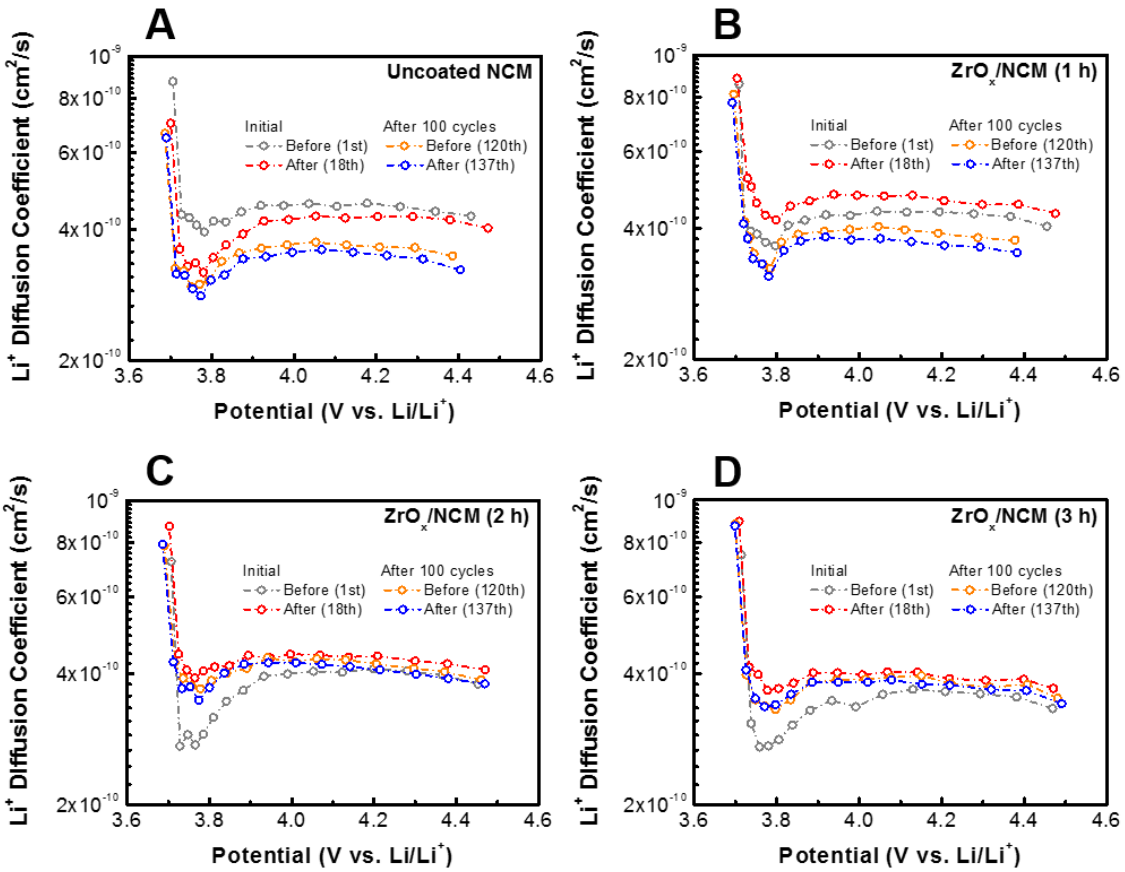

Fig. S4 Diffusion coefficient of Li ions (D_{Li}) measured using GITT at 4 selected cycles before and after the rate tests performed at 2 cycle regimes (initial and after 100 cycles) of uncoated (A) and ZrO_x-coated L333 for 1 (B), 2 (C), and 3 h (D).

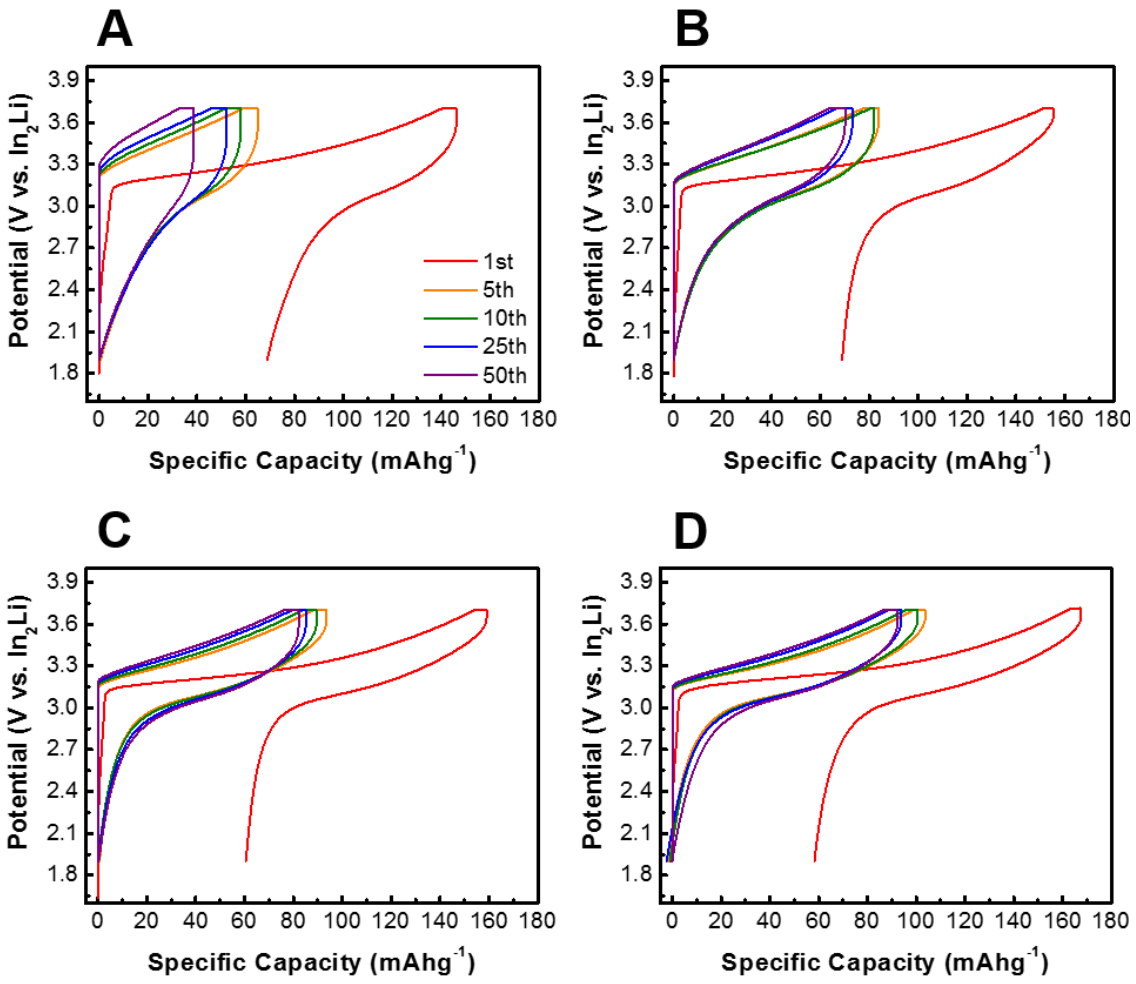

Fig. S5 Potential profiles evolved during 50 cycles for uncoated (A) and ZrO_x-coated L333 for 1 (B), 2 (C), and 3 h (D) charged/discharged under a Li_2S (77.5 mol %) + P_2S_5 (22.5 mol. %) solid-state electrolyte.

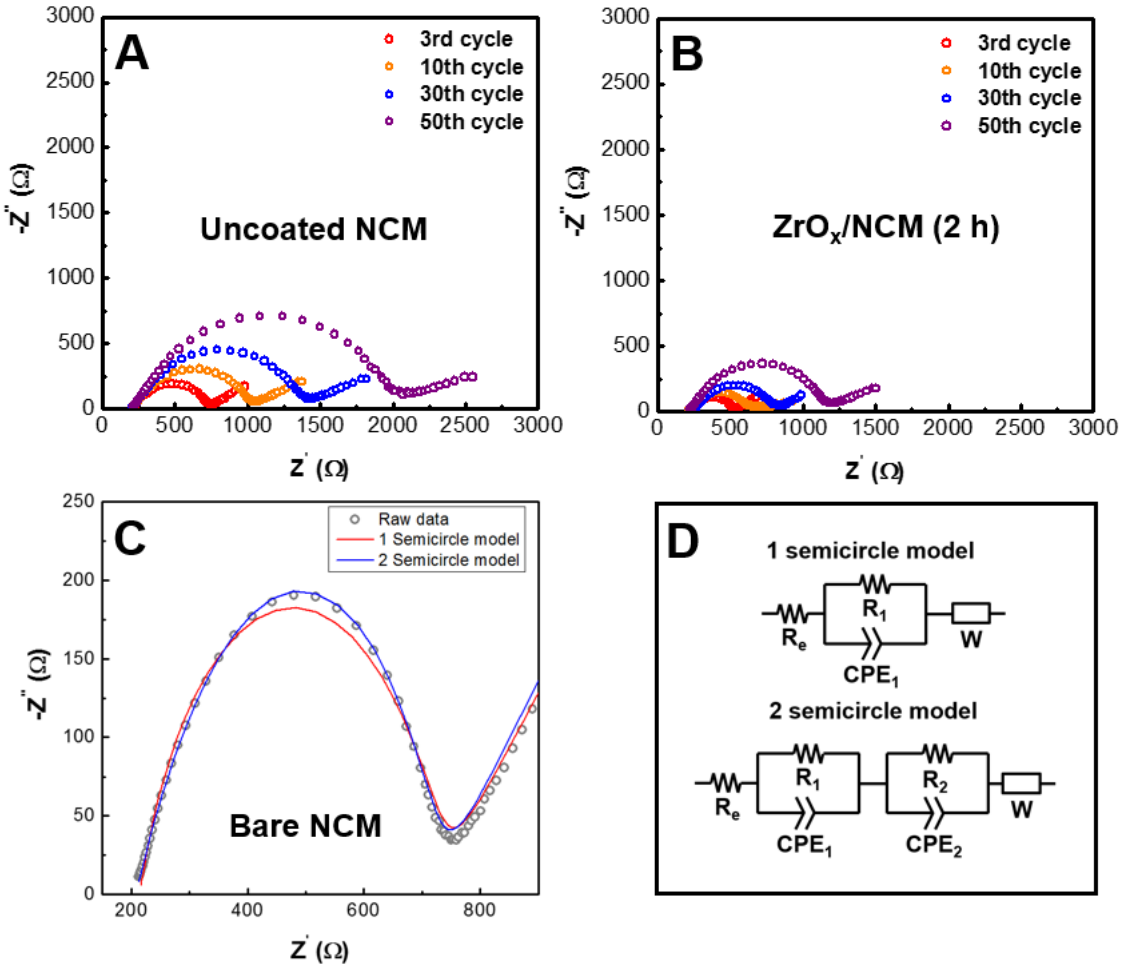

Fig. S6 Nyquist plots during cycling for uncoated (A) and ZrO_x-coated L333 (2 h) (B) measured at fully charged state at 3.7 V vs. In_2Li and cycled with inorganic solid-state electrolytes. (C) Nyquist plot (gray dot) and simulated curves with equivalent circuit model containing 1 semicircle (red solid line) and 2 semicircles (blue solid line).

Niquist plots of solid-state batteries were simulated using two semi-circle model with two constant phase elements (CPEs), which is identical with the model used to simulate the Niquist plots of cells cycled with liquid electrolytes. CPEs were introduced into the equivalent circuit model because the shape of observed semi-circles was deviated from the ideal shape, i.e., depressed semi-circle. The two

resistance components ($R_{surface}$ and R_{ct}) parallel with two CPEs correspond to resistance barriers arisen from the Li-deficient region developed in the electrolytes side (in the case of coated cathodes, ZrO_x layers are also accounted) and charge transfer process through interfaces between uncoated or coated active materials and solid electrolytes, respectively.

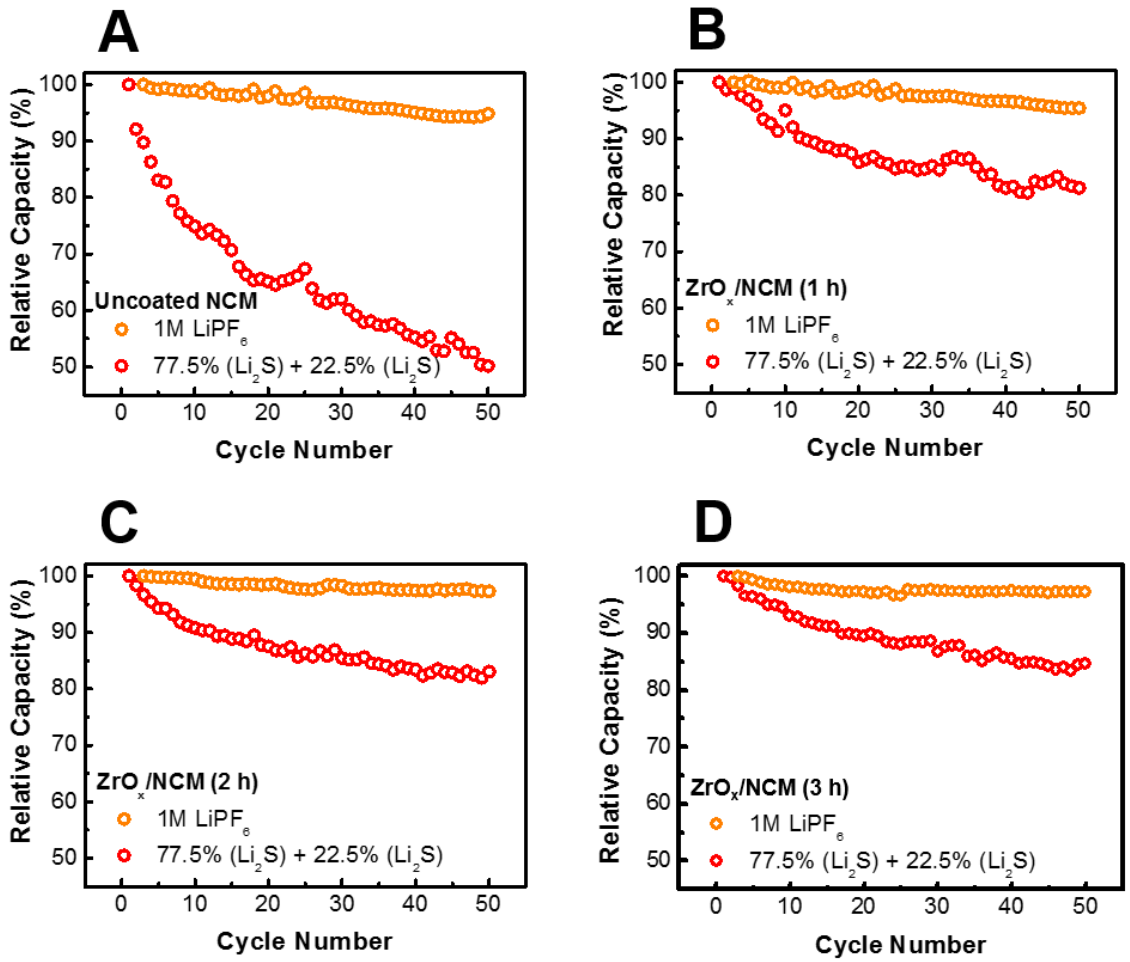

Fig. S7 Comparison of capacity retention during 50 cycles of uncoated (A) and ZrO_x-coated L333 electrodes for 1 (B), 2 (C), and 3 h (D) cycled with organic liquid (orange dots) and inorganic solid-state electrolyte (red dots). The relative capacity (%) was normalized by the 3rd and 1st discharge capacity of the electrodes cycled with liquid and solid electrolytes, respectively.

It is assumed that the relatively lower capacity and retention observed in the solid-state cell originated from not only the lower Li ion conductivity of SSE but also a combination of an undesired interfacial layer and the small contact area between the active material and SSE. The SSE powder makes a point contact with the active material, whereas the $LiPF_6$-based liquid electrolyte exhibits almost perfect wetting on the surface of active materials as well as pores in the electrodes.

Electrochemical energy storage can be initiated from only the interphase between active materials and electrolytes, and the smaller contact area in the all-solid-state cell leads to a lower specific capacity. In addition, considering the energy storage site of the layered-structure cathode, a facile and major pathway for Li ion through the cathode requires certain crystallographic spaces, i.e., an interslab space (a plane perpendicular to the c-axis). If the SSE power is attached to L333 with unfavorable crystallographic spaces, Li ions should be diffused into/form L333 through a detour path. In addition, products of the side reactions forming during cycling, e.g., SEI formation, can further impede the intercalation/deintercalation of Li into/from L333, and capacity loss with repeated cycling becomes severe because of the relatively low contact area and long diffusion length of Li. The most remarkable reduction in capacity and its retention from the liquid electrolyte-based cells was observed in the uncoated L333 electrodes (ESI, Fig. S7†), and the reduction was relieved with increasing sputtering time of the ZrO_x layer.

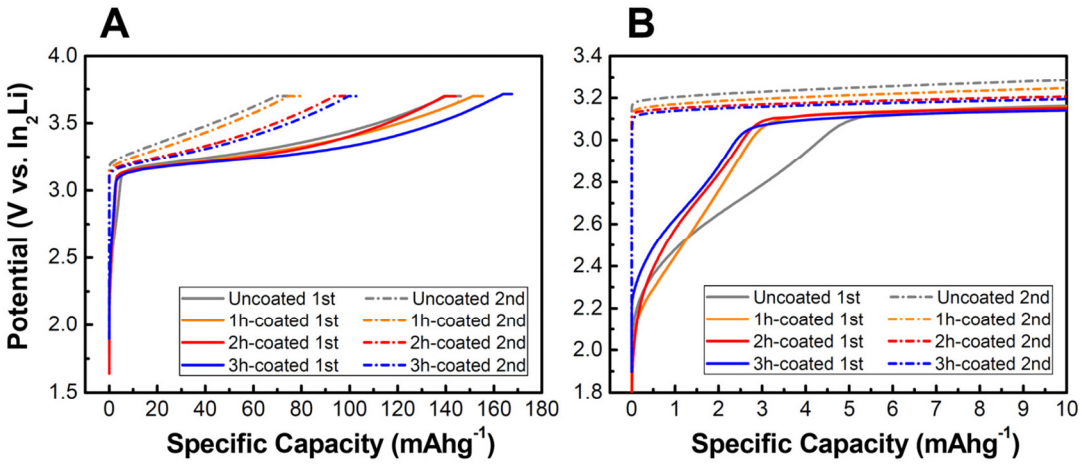

Fig. S8 (A) Potential profiles of uncoated and ZrO_x-coated L333 cathodes cycled with solid-state electrolyte of Li_2S (77.5 mol.%) + P_2S5 (22.5 mol.%) at 1st and 2nd cycles during charge process. (B) Magnified potential profiles of Fig. A.

Notes and references

1 I Belharouak, Y.-K Sun, and J Liu, *J. Power Sources*, 2003, **123**, 247–252.

2 T. Ohzuku, and Y. Makimura, *Chem. Lett.*, 2001, **7**, 642–643.

3 L. Q. Wang, L. F. Jiao, H. T. Yuan, J. Guo, M. Zhao, H. X. Li, and Y. M. Wang, *J. Power Sources*, 2006, **162**, 1367–1372.